Fracture phenomena of disordered media

Chung, Jim

6

OUTLOOK

The objective of this thesis is to present a computer simulation methodology to study effects of disorder on fracture phenomenon, in which microstructural features on a micrometer length scale are the most determining factor. A summary of the length scale involved so far is schematically presented in Figure 6.1. Starting with the results obtained so far the purpose of this chapter is to present an outlook for handling failure mechanism of highly porous ceramics on different length scales. In fact, our approach delineated in the preceding chapters focuses on a description of a single extruded particle, which is called an extrudate. Highly porous ceramics under investigation are used in the chemical industry as catalyst carriers and generally speaking a catalyst carrier should have a high porosity and small pores. But the pore size should not be too small because otherwise transport of the raw material is severely hampered. Decreasing the pore size of these materials will increase the specific area, but may also lead to conditional reactions, because the material may act as a molecular sieve. Besides these microstructural considerations, the materials must be able to operate in typical petrochemical conditions and must therefore have suitable mechanical properties in order to withstand the applied load under operation.

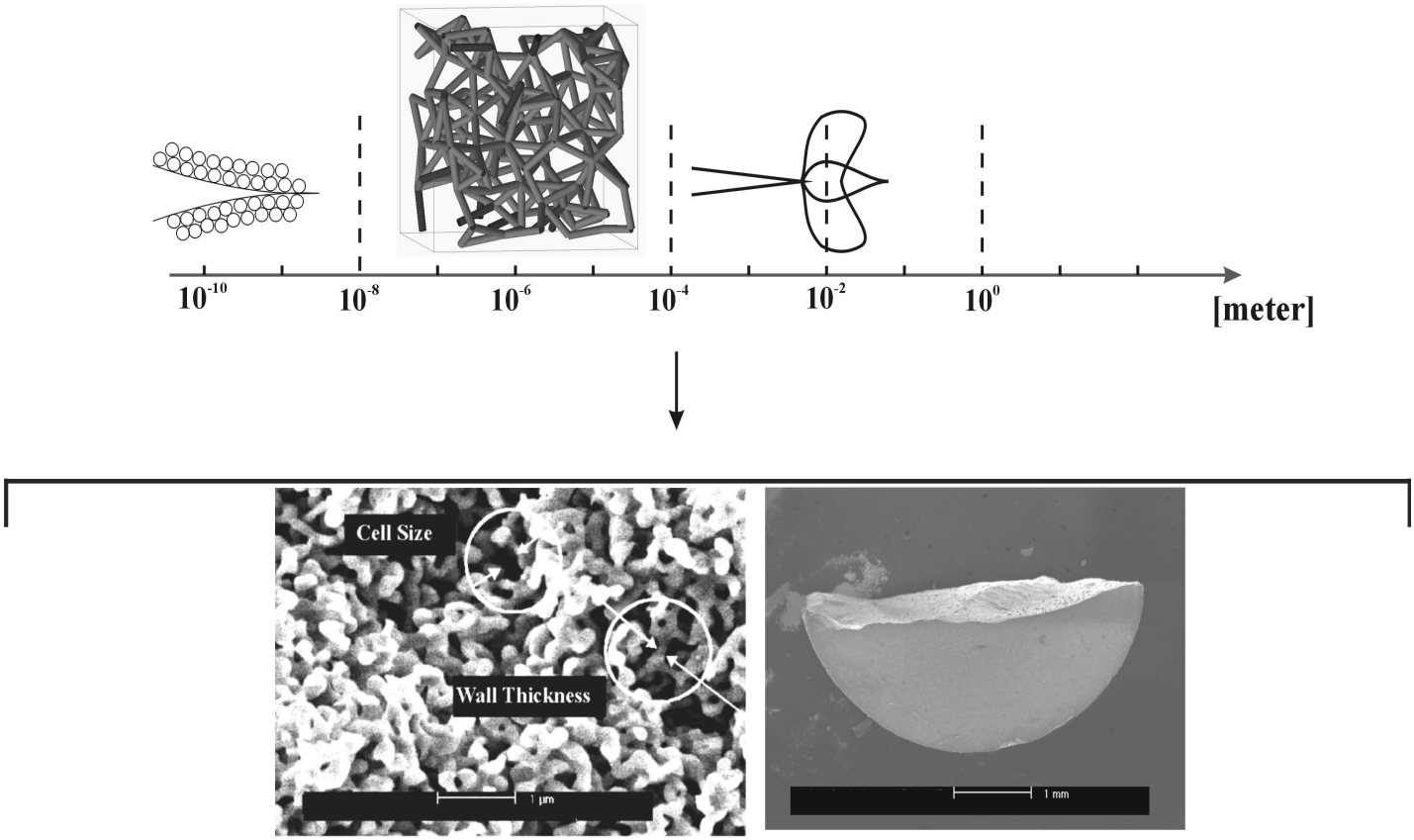

Figure 6.1. The various length scales involved; from an atomistic view on fracture, via a mesoscopic approach on a μm scale to a description based on classical fracture mechanics. The mesoscopic length scale is the focal point in this thesis. The SEM picture on the left shows the cell size and wall thickness in a SiO_2 extrudate, whereas on the right a broken extrudate is displayed (courtesy J.-j. Aué [6]).

Problems will arise when catalyst carriers at the bottom of the reactor crumble under the load of other carriers. This affects the flow through the reactor and efficiency of the process will diminish. Thus the mechanical properties of a collection of extrudates are of great importance to the practical performance of the carrier.

To access the strength of the catalyst carrier from an experimental point of view it is possible to measure the amount of attrition under specific loading conditions. To evaluate this behavior standardized tests were designed in the past in which the single particle strength was determined under specific test conditions. In this so-called Side Crushing Strength[1] test a single extrudate is slowly deformed uni-axially at a constant strain rate. The methodology described in this thesis refers to this experimental technique. Nevertheless, the strength of a single particle that is modeled has to be transferred to the behavior in a bulk of many extrudates. However, this is not a trivial case because the local forces between the particles in the bulk and the fracture criteria of individual particles are unclear. At the other end of the scale, phenomena on an atomic level may determine the failure characteristics of one single extrudate and these have to be mimicked in the physical parameters of a model for the meso-scale. This outlook will show some preliminary results of computer studies on other length scales than the mesoscopic length scale that was described in the previous chapters.

Let us start on the atomic scale or nanometer scale. Experimentally, on that scale the fracture surface can be studied by a microscopy technique called AFM, atomic force microscopy. The most commonly used detection technique in AFM is the optical lever mechanism, introduced in 1988 [2,3,4,5]. Here, a focused laser beam reflects from the end of a tilted cantilever. Attached to this cantilever is a tip. Each angular movement of this tip is amplified in the movement of the reflected laser beam. This beam tilt can easily and accurately be detected by a double- or quadruple split photodiode. This is a simple yet accurate technique, working in any medium that allows a cantilever to move and a laser beam to pass through. Like in most SPMs (scanning probe microscopy), scanning and positioning of tip and substrate are performed by piezoceramic actuators. Mostly the Z-direction is defined as being perpendicular to the average surface plane, the latter determining the XY-plane. With imaging, the combination of coordinates X,Y,Z and the signal is used to make a more or less topographic plot of the surface. This can be a strict XY-plane, in fact a constant Z-measurement. However, usually it is of more practical value to present a constant-interaction plot, as this forms a more natural definition of the local surface. In this case, the Z-positioning is varied in such a way that during XY-

movement, the force signal stays constant. This is simply implemented by comparing the detected signal to some reference value. In Figure 6.1a an experimental AFM height mode image of a SiO_2 based extrudate is presented [6, 7] whereas in Figure 6.1b a calculated image is displayed in which a void volume tip is used to move over a fracture surface of a computed fragment.

Theoretical and experimental analyses of AFM images can be used to scrutinize the scaling behavior of the surface roughness of brittle fracture making a connection to the mechanical behavior [8,9]. In particular the question can be raised whether the microstructure exhibits a fractal behavior. A modeling study using a random fuse network of fracture was presented by Hansen et al. [10], predicting universal scaling behavior of fracture surfaces (for a 2D simulation of the material) not depending on the microstructure. A fractal dimension D = 1.3 ± 0.1 is proposed with a corresponding Hurst exponent of 0.7. This scaling parameter has indeed been verified experimentally and was reported [11] for fracture of metals and also for some brittle materials[12]. Hansen et al.[10] also predicted disorder dependence for this universal scaling exponent. In the porous disordered materials experimentally investigated, the pore-size distribution represents the amount of disorder. This enabled us to study the effect of disorder on the scaling behavior of the fracture surface. These highly porous materials are built of clusters of colloidal particles and voids, which raise the question at which length scale the mechanical properties are determined. It may tell us what the determining and limiting factors are in the fracture processes of our materials. The fractal dimension can also be seen as a useful tool to characterize the spatial organization of a surface, an aspect that classical surface characterization techniques (RMS) cannot do in general. The fractal dimension marks the memory effect of the crack while creating the fracture surface. In fact, certain links can be made between scaling behavior of fracture surfaces and mechanical properties of materials.

The fractality comes into the description of the crack resistance force due to the surface energy term Γ. A self-affine fracture surface *h(r)* can be described at point r by:

$$h(r) \approx \left(\frac{r}{\xi} \right)^{H} \tag{6.1}$$

with the Hurst exponent 0 < H <1. It is assumed that the self-affine surface is fractal up to the correlation length ξ. At larger distances, the surface can be considered to be flat. The surface energy corresponding to open crack is:

$$\Delta E_s \cong 2\Gamma w \int^{a} \sqrt{1+\left(\frac{dh(r)}{dr} \right)^{2}}\, dr \tag{6.2}$$

and ΔE_s depends on the local slope of the self-affine fracture surface. The width of the specimen along the crack line is w and a is the crack length. Depending on the slope a new length scale r_c can be introduced in such a way that if r< r_c and $dh/dr >> 1$, the surface energy is approximated by:

$$\Delta E_s \cong 2\Gamma w a \quad \text{if } a > r_c \tag{6.3}$$

and

$$\Delta E_s \cong 2\Gamma w \left(\frac{a}{\xi} \right)^{H} \quad \text{if } a < r_c \tag{6.4}$$

In the former case, even at a length scale smaller than the correlation length, the surface free energy term is similar to the one needed for the creation of a flat surface, although the actual surface is rough. If $a<r_c$ the fracture toughness also depends on the correlation length and the fractal dimension. By equating the released elastic energy to the surface energy term, one can derive that the critical intensity factor for the fractal case, $K_{Ic}^{(F)}$, with $a<r_c$ reads:

$$K_{Ic}^{(F)} = K_{Ic}^{(0)} \sqrt{H}\, (\xi)^{-\frac{H}{2}} \tag{6.5}$$

where $K_{Ic}^{(0)}$ is the critical intensity factor for creating a flat surface. If the length scale r_c becomes larger than the correlation length ξ, the stress intensity factor in Eq. (6.5) depends only on ξ and not on H.

An interesting point is that with our modeling approach it would be possible to calculate H and the correlation length from simulated AFM images and to compare these with experimental ones. This is particularly useful because in numerous experiments the observed Hurst exponents H scatter in a wide range, because the correlation lengths vary [13]. For that reason, very controlled and accurate measurements and analysis are necessary to connect mechanical properties to the Hurst exponent [14].

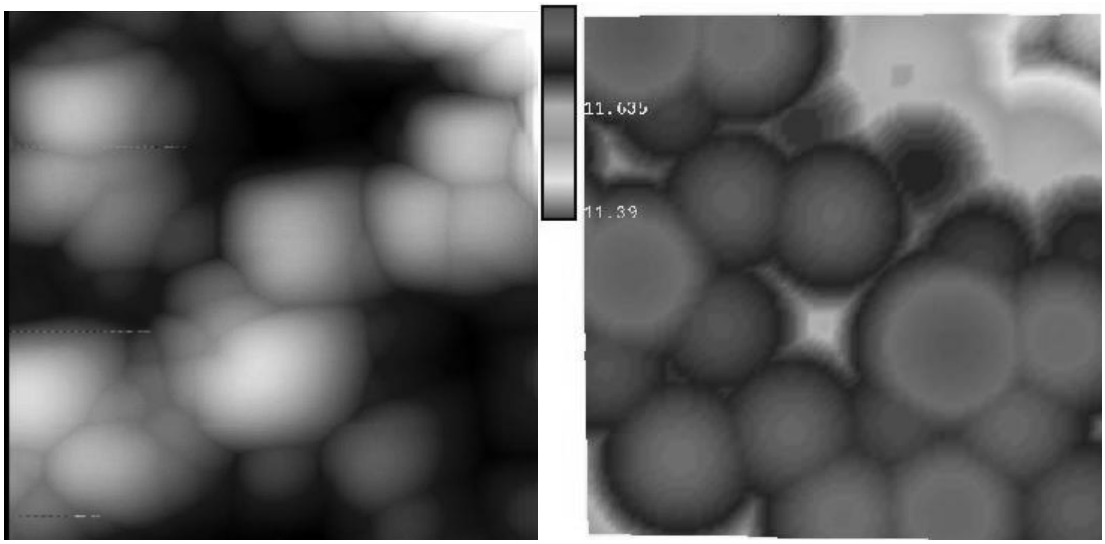

Figure 6.2. On the right side a computed AFM image from a tip across a fracture surface of our network. On the left side an experimental AFM image of the fracture surface of SiO_2 (courtesy B. Gabriels and J.-j. Aué).

If we look at crack propagation through a highly porous medium and assume that a crack propagating over an area l^2 will, on average, break t^2 cell walls, it can be derived [6,7] that the critical stress intensity factor becomes proportional to

$$K_{Ic}^{Porous} \sim \sqrt{D}\left(\frac{l}{l_p}\right)^{\frac{D-1}{2}} \tag{6.6}$$

where D is the fractal or self-similarity dimension of the crack surface and l_p is the size of the building block of the cell wall material.

Indeed, the existence of fractal law in fracture is reported so often that one can truly speak of 'Fractals everywhere' [15]. However, the fractal approaches to fracture phenomena need a rather delicate treatment. One of the first attempts to construct a mechanical model of a fractal crack was presented by Mosolov[16]. The stress intensity factor K_I^F of a fractal crack was derived in terms of the nominal stress σ, the macro-dimension of the crack a as

$$K_I^F \sim \sigma a^{H/2} \tag{6.7}$$

where $H=2-D$ and similar kinds of formulations are quite popular in literature. However, one should realize that in order to obtain formulae for the stress intensity factors within the framework of classical linear fracture mechanics, one must solve a boundary value problem for an elastic plane with a rectilinear cut. Therefore, strictly speaking to obtain K_I^F one has to solve the boundary value problem for an elastic plane with a fractal cut. To the best of our knowledge, even the mathematical formulation of the problem has not been presented in literature. Although the aforementioned equations can be useful in describing scaling phenomena of the fracture energy (i.e. for physical fractals, not for mathematical fractals) in an infinite solid, it has to be extended for a formulation of the size effect of fracture by considering the sample boundary in the formulation[17, 18].

Moving up in length-scale the fracture process of a single extrudate can be studied under different loading conditions. Side crushing, triple point and four point bending are examples of various loading conditions. The failure load and size effects may depend on the various loading conditions. A sphero-cylinder can be constructed in a computational study to represent a highly porous ceramic extrudate. Such a study is in particular relevant for a next step in length-scale, that is to say, towards the bulk-scale in which many extrudates interact. We take a large set of sphero-cylinders (see Figure 6.3) that span a

configuration space. The latter can be represented by a three-body density function (triplet correlation function), which is depicted in Figure 6.4 .

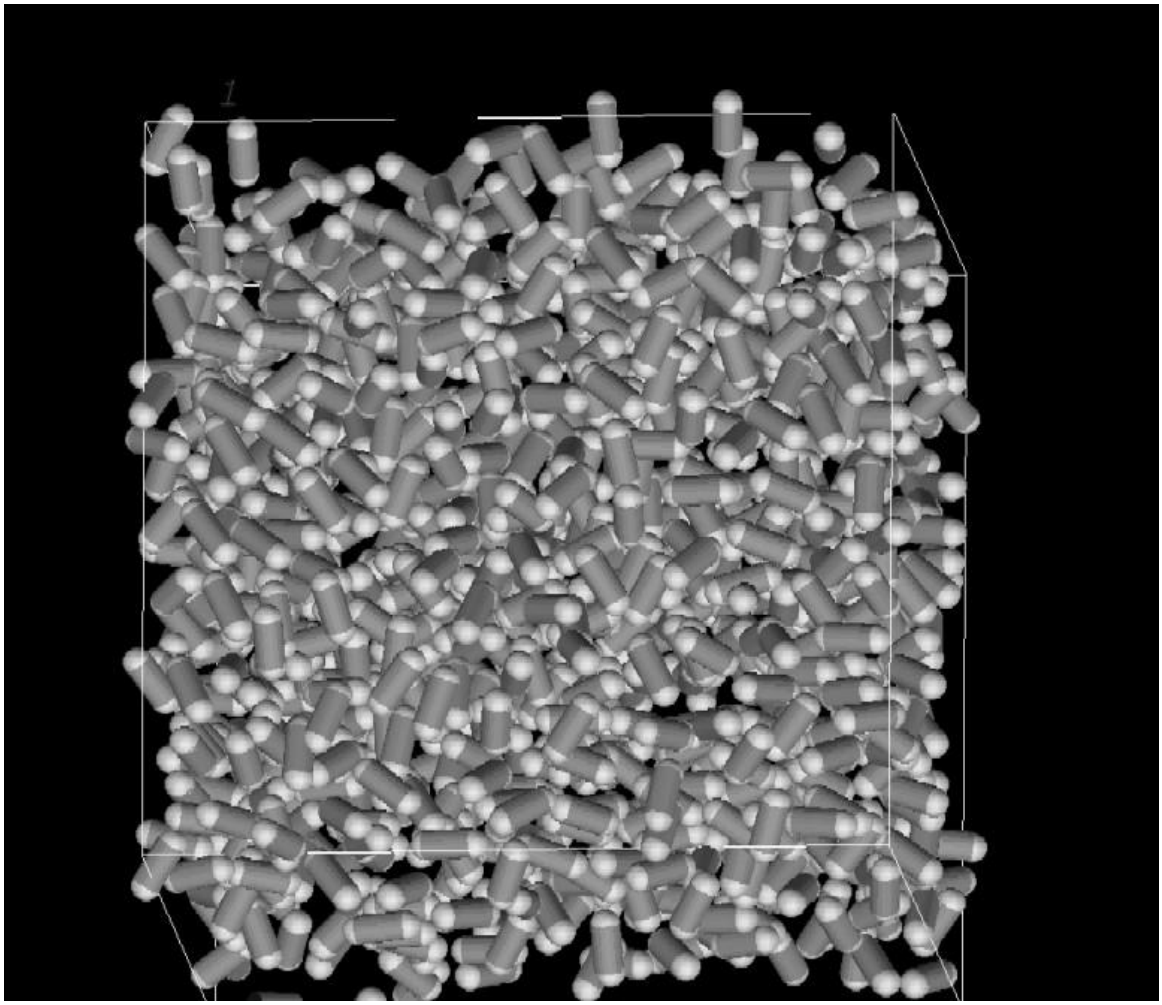

Figure 6.3. Snapshot containing 1000 sphero-cylinders in a periodic box.

In Figure 6.4 the color indicates the specific value of the distribution and the relative angle on the left runs from 0 to π/4 whereas the other axis represents the relative distance to the reference extrudate.

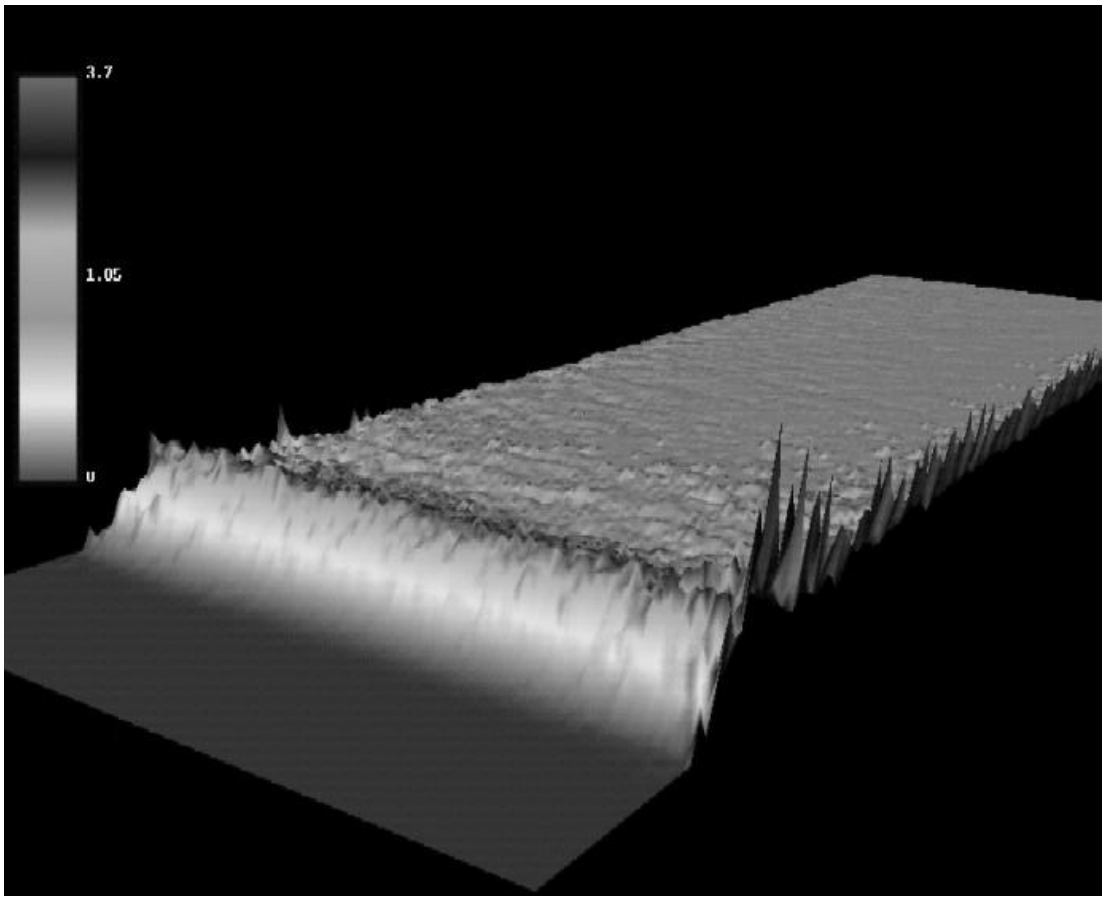

Figure 6.4. The angle distribution function (normalized) along the relative distance between the extrudates. The color indicates the specific value of the distribution and the relative angle on the left runs from 0 to $\pi/4$ whereas the other axis represents the relative distance to the reference extrudate.

From the box of sphero-cylinders a distribution of contact points can be obtained that somehow will determine the local failure characteristics. If extrudates are oriented along one side of the box the relevant failure mechanism would be side crushing. By varying the ratio of the length/diameter of the sphero-cylinders the number of contact points will be affected and therefore the failure. As a result it is also possible to transform the orientation space into some sort of a 'failure space'.

In the primary studies a hard wall box containing 1000 moving extrudates is constructed. In this case the extrudates are modeled like 2 overlapping spheroids. To study influences of the orientation distributions the walls along the vertical axis were moved towards each other. The change in orientation of the sphero-cylinders by the walls and compression can be noticed in Figure 6.5.

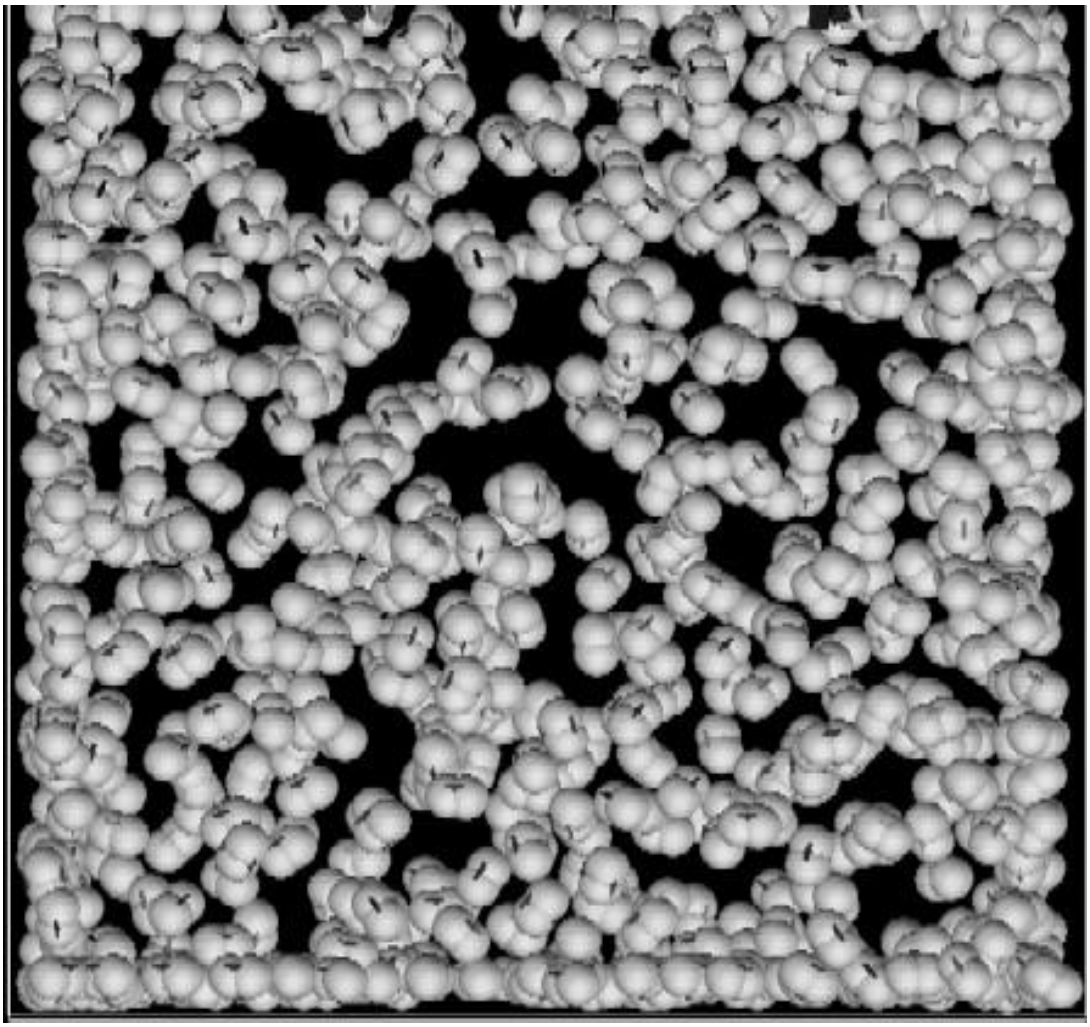

Figure 6.5a.

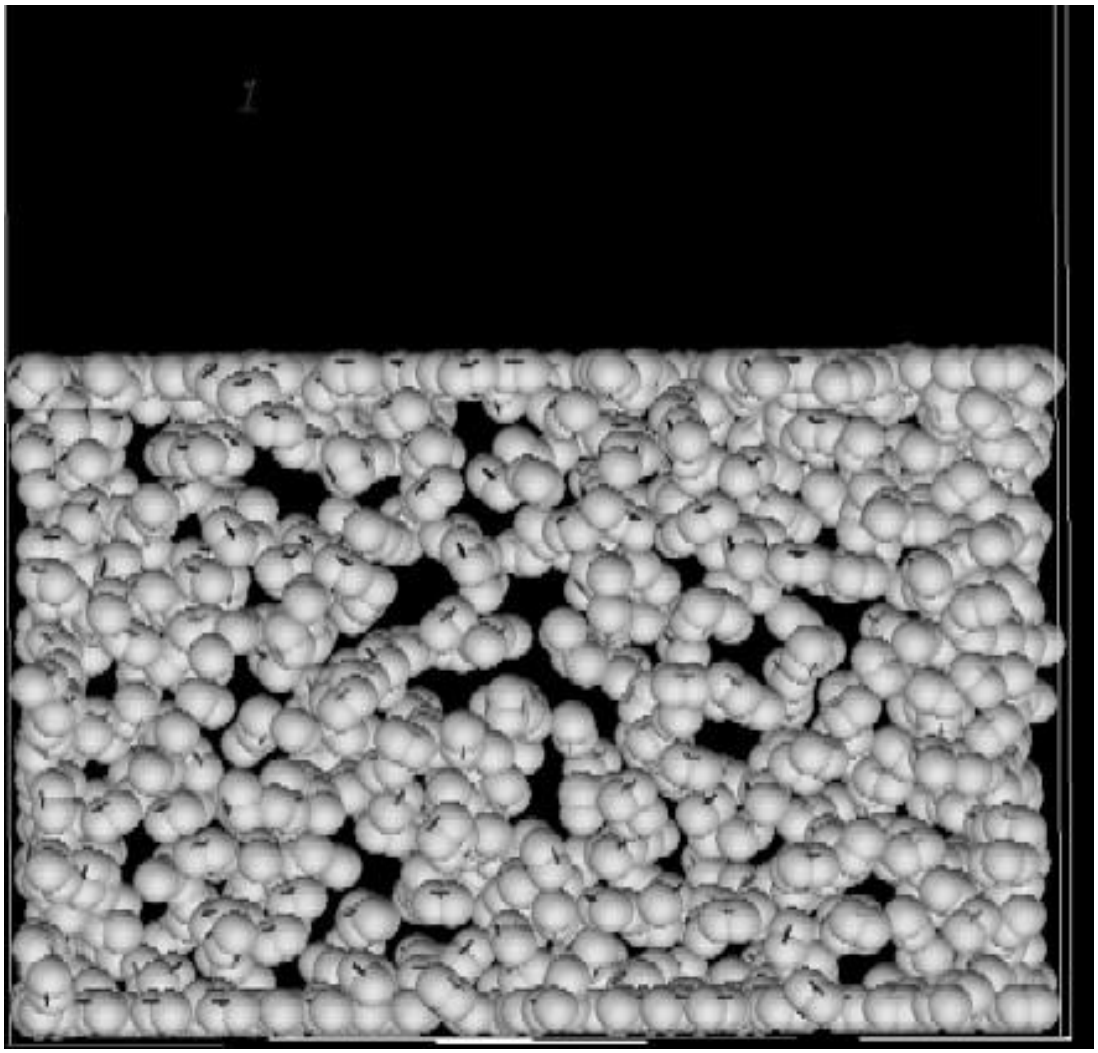

Figure 6.5b.

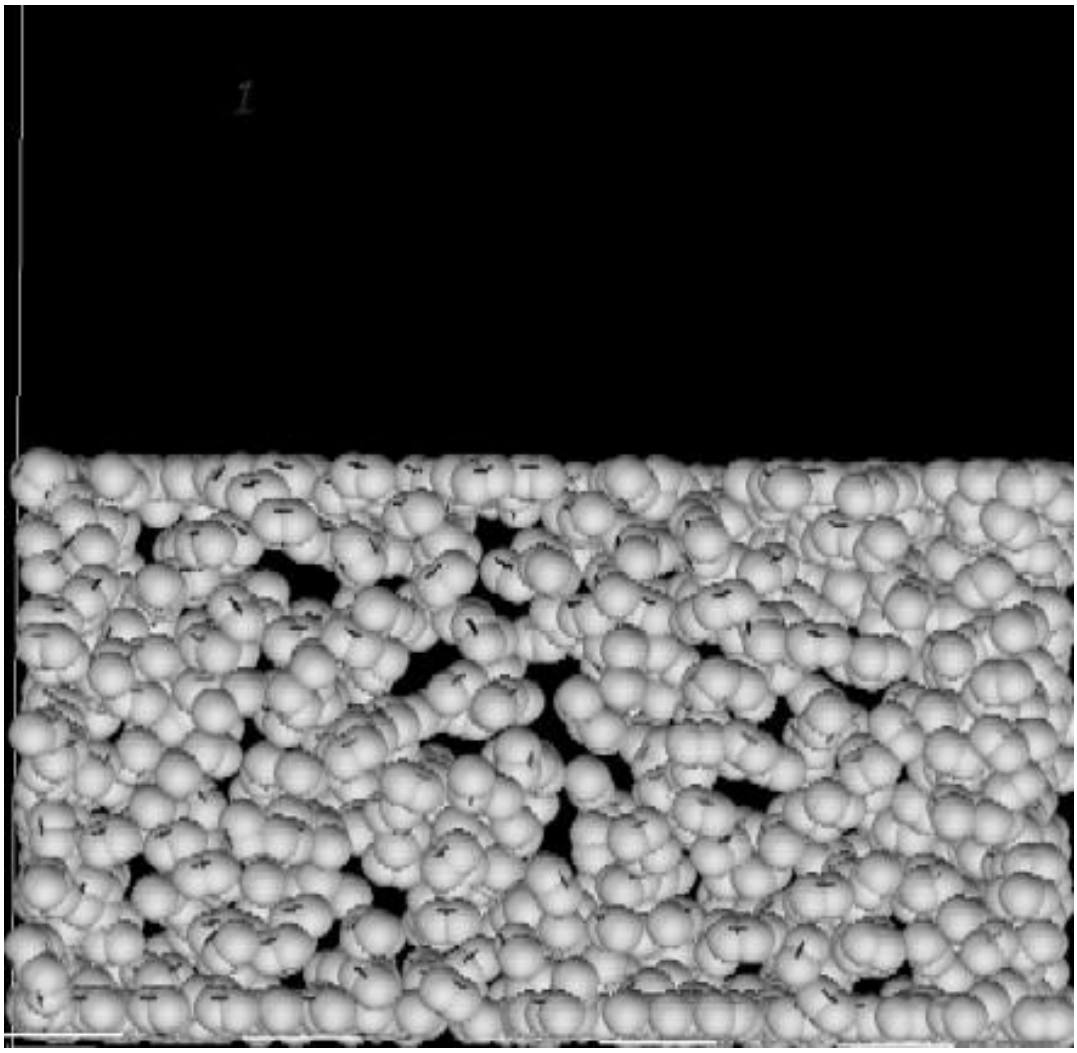

Figure 6.5c.

Figure 6.5. From top (a) to bottom (c) : the process of compression on a collection of extrudates modeled as overlapping spheres.

With this concise preview of preliminary studies, the author intends to provide the reader a glimpse of the attractive possibilities to gain further physical insight with a Computational Materials Science approach into the "failure stress of highly porous ceramics".

REFERENCES

1 I.C. van den Born, A. Santen, H.D. Hoekstra, J.Th.M. De Hosson, Phys. Rev. B, 43, 3794 (1991).

2 G. Meyer, N. M. Amer, Appl. Phys. Lett. **53**, 1045 (1988).

3 S. Alexander, l. Hellemans, O. Marti, J. Schneir, V. Eilings, P.K.Hansma, M. Longmire, J. Gurley, J. Appl. Phys. **65**, 164 (1989).

4 J.W.J. Kerssemakers and J.Th.M. De Hosson , J.Applied Physics, 83, 3444(1998) and 82,3763 (1997).

5 J.W.J. Kerssemakers, Concepts of interactions in local probe microscopy, Thesis, University of Groningen, 1997.

6 J.-j. Aué, Fractals and fracture, Thesis, University of Groningen, 1997.

7 J.–j Aué and J.Th.M. De Hosson Appl Phys. Letters. 71 ,1347(1997).

8 J.C. Charmet, S. Roux, E. Gyon, Disorder and fracture, Plenum Press, 1989

9 J.Y. Thompson, K.J. Anusavice, B. Balasubramaniam, J.J. Mecholsky jr., J. Am. Ceram. Soc., 78, 11, 3045-49 (1995).

10 A. Hansen, E. Hinrichsen, S. Roux, Phys. Rev. Let., 66, 19, 2476 (1991).

11 E. Bouchaud, G. Lapasset, J. Planès, Eurphys. Let., 13, 1, 73(1990).

12 A. Hansen, S. Roux, Phys. Rev. Let., 69, 2, 213-15(1992).

13 K.J. Måløy, A. Hansen, E.L. Hinrichsen, S. Roux, Phys. Rev. Lett. , 68, 213 (1992).

14 P.M. Duxbury, Statistical models for the fracture of disordered media, H.J. Herman, S. Roux (eds.), 189, Elsevier, 1990.

[15] M. Barnsley, Fractals everywhere, Academic Press, Boston, USA, 1988.

[16] A.B. Mosolov, Sov.Phys.-Tech.Phys. 61,57 (1991).

[17] F.M. Borodich, Nonlinear analysis, 30, 409 (1997).

[18] F.M. Borodich, Fracture scaling, Ed. Z. Bažant, Y. D.S. Rajapakse, Kluwer Academic Pub., Dordrecht, 1999.